Arabian Journal of Chemistry (2015) xxx, xxx–xxx

King Saud University

Arabian Journal of Chemistry

www.ksu.edu.sa
www.sciencedirect.com

ORIGINAL ARTICLE

Oxidative dehydrogenation of *n*-octane over a vanadium–magnesium oxide catalyst: Influence of the gas hourly space velocity

Elwathig A. Elkhalifa [a,b,*], **Holger B. Friedrich** [b]

[a] *Department of Chemistry, Faculty of Science, University of Khartoum, Khartoum, Sudan*
[b] *School of Chemistry and Physics, University of KwaZulu-Natal, Durban 4000, South Africa*

Received 18 November 2014; accepted 30 March 2015

KEYWORDS

VMgO;
Dehydrogenation;
Octenes;
C8 aromatics

Abstract Oxidative dehydrogenation (ODH) of *n*-octane was carried out over a vanadium–magnesium oxide catalyst in a continuous flow fixed bed reactor. The catalyst was characterized by ICP–OES, powder XRD and SEM. The catalytic tests were carried out at different gas hourly space velocities (GHSVs), viz. 4000, 6000, 8000, and 10,000 h^{-1}. The best selectivity for octenes was obtained at the GHSV of 8000 h^{-1}, while that for C8 aromatics was attained at the GHSV of 6000 h^{-1} at high temperatures (500 and 550 °C). The catalytic testing at the GHSV of 10,000 h^{-1} showed the lowest activity, while that at the GHSV of 4000 h^{-1} consistently showed the lowest ODH selectivity. Generally, the best ODH performance was obtained by the catalytic testing at the GHSVs of 6000 and 8000 h^{-1}. No phasic changes were observed after the catalytic testing.

1. Introduction

Because of the increasing demand for alkenes and aromatics, there is a growing tendency in the petrochemical industry to the usage of alkanes as feedstock to produce these compounds. In fact, the dehydrogenation of long-chain alkanes to produce value-added products, such as alkenes and aromatics, is an important reaction from both scientific and industrial points of view (Fung and Wang, 1991; Meriaudeau et al., 1994; Jongpatiwut et al., 2003). Moreover, it converts the low octane number *n*-alkanes into the high octane number alkenes, dienes, and aromatics. For *n*-octane, catalysts based on platinum, which is incorporated on a suitable support, were commonly used in this type of *n*-octane activation, e.g. platinum supported in zeolites (Jongpatiwut et al., 2003), silica (Shi and Davis, 1995), silicalite (Meriaudeau et al., 1994), and alumina (Sivasanker and Padalkar, 1988). Catalysts based on titania, zirconia, hafnium oxide, and molybdenum oxide were also used (Trunschke et al., 2001; Szechenyi and Solymosi, 2006). In these studies, mainly non-oxidative, small amounts of octenes were formed; selectivities of 1–6% to the octenes were

* Corresponding author at: Department of Chemistry, Faculty of Science, University of Khartoum, Khartoum, Sudan. Tel.: +249 912982467.
E-mail addresses: wathigae@yahoo.com, elwathigae@uofk.edu (E.A. Elkhalifa), friedric@ukzn.ac.za (H.B. Friedrich).
Peer review under responsibility of King Saud University.

ELSEVIER Production and hosting by Elsevier

http://dx.doi.org/10.1016/j.arabjc.2015.03.017
1878-5352 © 2015 The Authors. Production and hosting by Elsevier B.V. on behalf of King Saud University.
This is an open access article under the CC BY-NC-ND license (http://creativecommons.org/licenses/by-nc-nd/4.0/).

Please cite this article in press as: Elkhalifa, E.A., Friedrich, H.B. Oxidative dehydrogenation of *n*-octane over a vanadium–magnesium oxide catalyst: Influence of the gas hourly space velocity. Arabian Journal of Chemistry (2015), http://dx.doi.org/10.1016/j.arabjc.2015.03.017

obtained (Jongpatiwut et al., 2003), and, interestingly, no styrene was reported (Jongpatiwut et al., 2003; Szechenyi and Solymosi, 2006).

For the production of olefins and aromatics, oxidative dehydrogenation (ODH) represents a potential alternative for the currently used non-oxidative dehydrogenation, as no thermodynamic equilibrium limitations are expected. Moreover, in the ODH, chances for a catalyst's deactivation may be minimized as the possibility for coke formation will be lower. The main obstacle in the ODH of alkanes is that the total oxidation products (carbon oxides) are thermodynamically more stable than the dehydrogenation products (olefins and aromatics). The great challenge, therefore, is to stop the reaction at intermediate stages (formation of olefins and aromatics), and not allow it to proceed further to form the thermodynamically stable carbon oxides (undesirable products). In this context, the reactants' adsorption and products' desorption are important steps that affect both the catalyst's activity and selectivity (Thomas and Thomas, 1997; Bowker, 1998). The selectivity in alkane oxidation is influenced by the residence time of the molecules on the catalyst's surface (Kung and Michalakos, 1993). Although the residence time of the reactants and the formed molecules is believed to be affected by catalyst's properties such as the acid-base character (Kung and Michalakos, 1993), factors such as the gas hourly space velocity (GHSV) will also have impacts on the residence time, and will hence affect the catalyst's performance.

In catalytic partial oxidation, optimization of the catalytic reaction with regard to variables such as reactor design, fuel/oxygen ratios, and contact time is important (Schmidt et al., 1994; Hodnett, 2000). In this partial oxidation, long contact times (low GHSV) will favour the formation of the thermodynamic equilibrium products (combustion products). Short contact times, on the other hand, will not give sufficient time for the reactants on the catalyst's surface to react, and thereby lower the activity of the catalyst. Moreover, short contact times (high GHSV) are likely to enhance the homogeneous reactions, which will probably lower the selectivity to the ODH products. Thus, contact time is an important variable that needs to be optimized for a given catalytic system. We have reported on the oxidative dehydrogenation of *n*-octane over VMgO catalysts (Elkhalifa and Friedrich, 2010, 2011, 2014); in these studies, reasonable selectivities for octenes and C8 aromatics were obtained. In the current report, the oxidative dehydrogenation of *n*-octane was carried out at different contact times over a VMgO catalyst, in a bid to affect the catalyst's activity and the selectivity pattern to different products. The contact time was influenced by changing the gas hourly space velocity (GHSV), i.e. by changing the flow rates of all the components of the reactant mixture.

2. Experimental

2.1. Synthesis and characterization

The magnesium oxide and the vanadium–magnesium oxide catalyst (VMgO) were synthesized by procedures similar to those outlined in (Elkhalifa and Friedrich, 2010). Thus, for the synthesis of the VMgO catalyst, 9.139 g of MgO was impregnated with around 800 ml of a hot aqueous solution that contained 1.931 g of ammonium vanadate; this is to give a nominal V_2O_5 concentration of 15% of the combined V_2O_5 and MgO. The resultant mixture was heated, while magnetically stirred, till a paste was formed. The paste was then transferred to a porcelain crucible and left overnight in an oven operated at 120 °C. The catalyst so-obtained was ground, homogenized, and was then calcined at 550 °C for 5 h. For the catalyst characterization, inductively coupled plasma optical emission spectroscopy (ICP–OES), powder X-ray diffraction (XRD), and scanning electron microscopy (SEM) techniques were performed on both the fresh and the used catalysts. ICP–OES was carried out using an Optima 5300 DV PerkinElmer Optical Emission Spectrometer. X-ray diffractograms were recorded on a Philips PW1050 Diffractometer equipped with a graphite monochromator and operated at 40 kV and 40 mA. The source of radiation was Co Kα and all data were captured by a Sietronics 122D automated microprocessor. The diffraction line at 2θ equal 50° was used to estimate the crystallite size (using the Scherrer equation). SEM images were obtained by using a LEO 1450 Scanning Electron Microscope. The catalyst samples that were used for obtaining these SEM images were coated with gold using a Polaron SC Sputter Coater.

2.2. Catalytic studies

The catalytic testing was performed in a continuous flow fixed bed reactor. The reactor tube was stainless steel with an inner diameter of 10 mm. The catalyst volume was 1 mL (ca. 0.45 g), and the catalyst pellet sizes were between 600 and 1000 μm. The catalyst was placed between two layers of glass wool and the rest of the reactor tube was packed with carborundum. The temperature of the catalyst bed was monitored with a coaxially centred thermocouple that was placed in the middle of the catalyst's bed. Air was used as an oxidant, and nitrogen as a make-up gas to obtain the required total flows. The flow rates of the air and the nitrogen were controlled by ABB rotameters. *n*-Octane was delivered to the reactor system by a LabAlliance Series II HPLC pump. The liquid products that came out of the reactor system were collected in a stainless steel vessel cooled to about 2 °C. The total volume of the gas that came out of the reactor system was measured by a Ritter Drum-Type Gas Metre. The catalytic tests were carried out at gas hourly space velocities (GHSVs) of 4000, 6000, 8000, and 10,000 h^{-1}, which correspond to the total flows of 67, 100, 134, and 167 ml/min, respectively. This corresponds to *n*-octane/air/nitrogen flow rates of 6/36/25, 9/54/37, 12/72/50, and 15/90/62 (ml/min) for the GHSVs of 4000, 6000, 8000, and 10,000 h^{-1}, respectively. The concentration of the *n*-octane in the gaseous mixture was, therefore, constantly kept at 9% (v/v). The products of the catalytic tests were analysed by a Perkin–Elmer Clarus 500 Gas Chromatograph equipped with an FID and a TCD. The FID was attached to a PONA column and was used for the quantification of the organic products. The TCD, on the other hand, was connected to a Carboxen 1006 PLOT column and was used for the quantification of the carbon oxides. The amount of water that was formed by the catalytic tests in both the organic and aqueous layers was determined by an 870 KF Titrino plus (Metrohm) Karl Fischer Titrator. Conversion and selectivity were calculated on a carbon basis, and all experiments were carried out in duplicate (carbon balances were in the range of 97–101%).

Please cite this article in press as: Elkhalifa, E.A., Friedrich, H.B. Oxidative dehydrogenation of *n*-octane over a vanadium–magnesium oxide catalyst: Influence of the gas hourly space velocity. Arabian Journal of Chemistry (2015), http://dx.doi.org/10.1016/j.arabjc.2015.03.017

3. Results and discussion

3.1. *n*-Octane conversion at different GHSVs

For the catalytic testing over the VMgO catalyst at the GHSVs of 6000, 8000, and 10,000 h^{-1} (Fig. 1), the general trend (except at 400 °C) was that the *n*-octane conversion decreases as the GHSV increases; this is consistent with the argument that a slow flow rate gives a good chance for the *n*-octane to be converted. This trend was also exhibited by the tests at the GHSV of 4000 h^{-1} at low temperatures (350 and 400 °C), but disturbed at higher temperatures (450–550 °C); especially at 550 °C where the conversion was noticeably low compared to the previous temperatures at this GHSV, and also to the other GHSVs. This is probably due to some sort of mass transfer problems at this low flow rate; in support of this, it is reported that under the conditions of mass transfer limitations, both catalyst' activity and selectivity will be lowered (Bhasin et al., 2001).

3.2. Product selectivity at different GHSVs

As Fig. 2 shows, selectivity to octenes does not change much as the temperature rises. However, the best selectivity to octenes was obtained at the GHSV of 8000 h^{-1}, while the lowest selectivity was observed at the GHSV of 4000 h^{-1}. The formation of the C8 aromatics (ethylbenzene, styrene, and xylene) only starts at 400 °C (Fig. 3). The catalytic test at the GHSV of 4000 h^{-1} shows the lowest selectivity to C8 aromatics, while the test at the GHSV of 6000 h^{-1} gives the highest selectivity at the temperatures 500 and 550 °C. However, selectivities to C8 aromatics were comparable at 400 and 450 °C for the GHSVs of 6000, 8000, and 10,000 h^{-1}.

For the carbon oxides (Fig. 4), the test at the GHSV of 4000 h^{-1} continuously shows the highest selectivity towards these combustion products. The lowest formation of carbon oxides was shown by the tests at the GHSV of 8000 h^{-1} at 400 and 450 °C, and by the tests at the GHSV of 6000 h^{-1} at 500 and 550 °C. The low selectivity towards ODH products along with the high formation of carbon oxides at the GHSV of 4000 h^{-1} may indicate that there was a significant contribution from the secondary combustion at this low flow

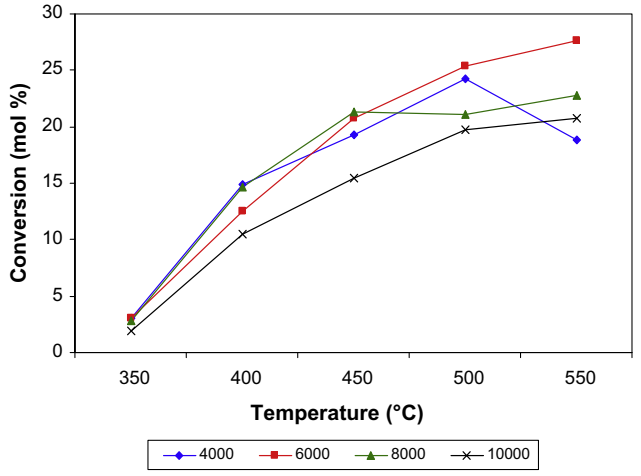

Figure 1 *n*-Octane conversion at different GHSVs (h^{-1}).

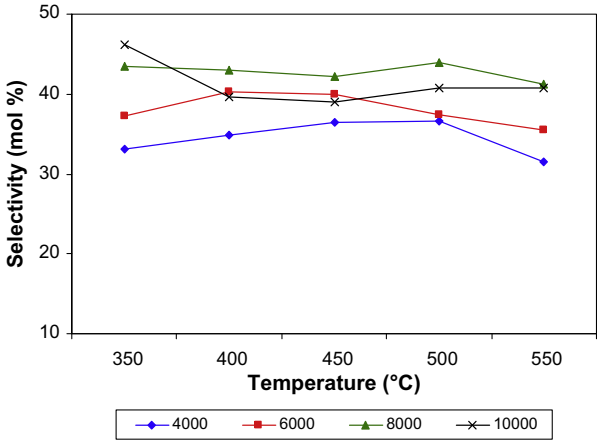

Figure 2 Selectivity to octenes at different GHSVs (h^{-1}).

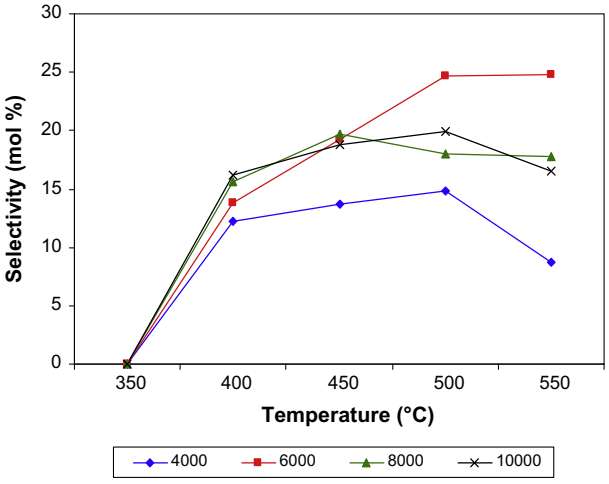

Figure 3 Selectivity to C8 aromatics at different GHSVs (h^{-1}).

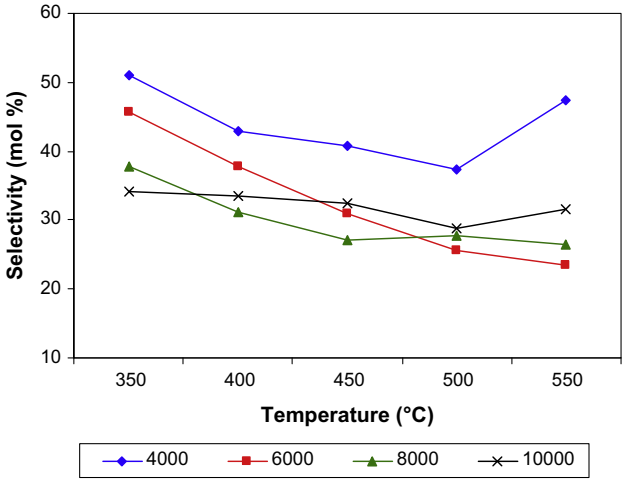

Figure 4 Selectivity to carbon oxides at different GHSVs (h^{-1}).

Please cite this article in press as: Elkhalifa, E.A., Friedrich, H.B. Oxidative dehydrogenation of *n*-octane over a vanadium–magnesium oxide catalyst: Influence of the gas hourly space velocity. Arabian Journal of Chemistry (2015), http://dx.doi.org/10.1016/j.arabjc.2015.03.017

rate. Under these conditions, the formed products were likely to be strongly adsorbed (relative to the other GHSVs) on the catalyst's surface, and as proposed in Kung and Michalakos, (1993); Blasco and Lopez Nieto, (1997); Bhasin et al., (2001), this resulted in a decrease in the ODH selectivity coupled with an increase in the selectivity to COx. Interestingly, as the temperature increases, there is a general increase in the C8 aromatics selectivity, which coupled with a decrease in the COx selectivity (Figs. 3 and 4). This may be attributed to the stability of the aromatic compounds which provides an energetically favourable pathway for the reaction, which in turn lowers the selectivity to COx; the same reverse relation was observed when VMgO catalysts with different vanadium loadings were employed in the dehydrogenation of *n*-octane (Elkhalifa and Friedrich, 2010). The formation of cracked products, as Fig. 5 displays, becomes significant, ≈3–7%, only at higher temperatures (500 and 550 °C). In this context, it is notable that the VMgO system maintained its low tendency towards the formation of cracked products (Blasco et al., 1995; Dejoz et al., 1999).

The formation of the dehydrogenation products will produce water as a by-product if these reactions proceed oxidatively, whereas hydrogen will be generated if these reactions take place non-oxidatively (Mamedov and Cortes Corberan, 1995). For the catalytic testing at the different GHSVs, the percentage of water that was practically produced relative to the total amount of water that should theoretically be formed if these reactions were entirely oxidative was calculated at the temperatures 450 and 500 °C. These percentages were in the range of 91–95% for the tests at the GHSVs of 10,000, 8000, 6000 h^{-1}, and were around 81% for the test at 4000 h^{-1}. This indicates that the products' formation by the catalytic testing was predominantly oxidative; however, a relatively higher contribution from the non-oxidative reactions may be suggested for the test at the GHSV of 4000 h^{-1}.

3.3. The production of 1-octene and styrene

High demand exists for 1-octene and styrene, as they are valuable products in the polymers industry. The formation of these products was, therefore, given especial consideration in this study. The yield of 1-octene (Table 1) was higher at the GHSV of 8000 h^{-1} for the temperatures 450 and 500 °C; however, as Table 1 shows, the GHSV of 6000 h^{-1} recorded the highest yield to 1-octene at higher temperatures (500 and 550 °C). The highest styrene yield (Table 2) was recorded at the GHSV of 6000 h^{-1} for the temperatures 500 and 550 °C (3.6 and 3.7, respectively).

Table 1 The yield of 1-octene at different temperatures (°C) and GHSVs (h^{-1}).

GHSV	T (°C) →	350	400	450	500	550
4000		0.3	1.7	2.1	2.4	1.4
6000		0.3	1.6	2.4	2.6	2.5
8000		0.3	1.9	2.5	2.4	2.2
10,000		0.2	1.3	1.7	2.1	2.1

Table 2 The yield of styrene at different temperatures (°C) and GHSVs (h^{-1}).

GHSV	T (°C) →	350	400	450	500	550
4000		0.0	1.0	1.3	1.7	0.4
6000		0.0	1.0	2.3	3.6	3.7
8000		0.0	1.3	2.3	1.9	1.9
10,000		0.0	1.0	1.6	2.0	1.5

3.4. Catalysts characterization

Catalysts characterization was aimed at investigating any phasic or morphological changes that may have occurred as a result of the catalytic tests. The elemental composition was very similar for both the used and the fresh catalysts (V_2O_5 percentage out of the combined V_2O_5 and MgO was 15.9%). Moreover, no phasic changes were observed after the catalytic tests, as shown by the XRD results (Fig. 6). As was the case for

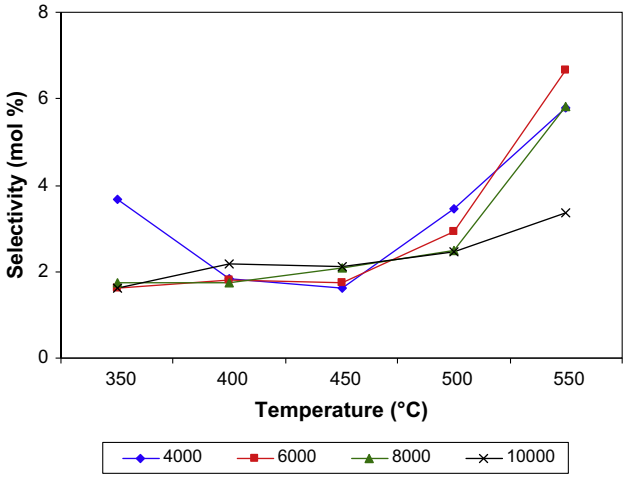

Figure 5 Selectivity to cracking products at different GHSVs (h^{-1}).

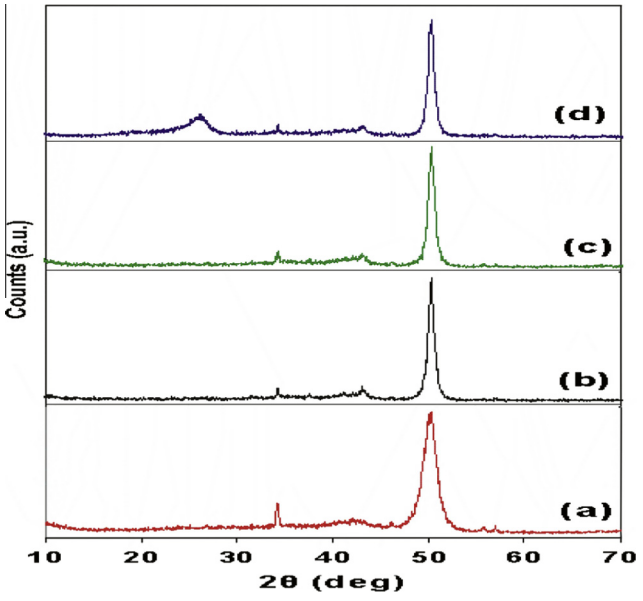

Figure 6 XRD diffractograms of: (a) fresh catalyst, (b), (c), and (d) are for the used catalysts at the GHSV of 10,000, 8000, and 4000 h^{-1}, respectively.

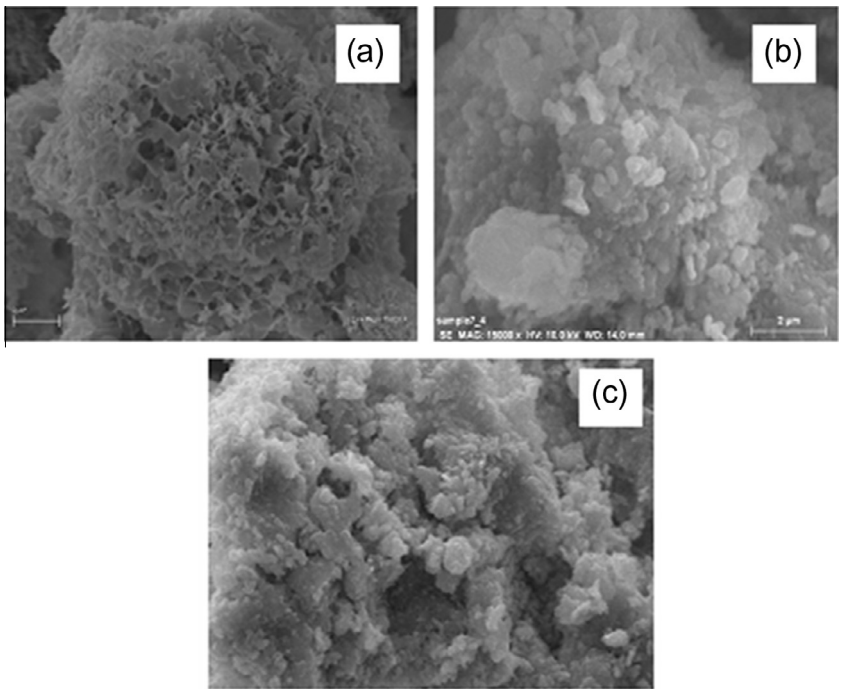

Figure 7 SEM images of: (a) fresh catalyst, (b) and (c) are for the used catalysts at the GHSV of 4000 and 10,000 h^{-1}, respectively.

the fresh catalyst, the only crystalline phases detected after the catalytic testing were magnesium oxide and magnesium orthovanadate. According to the assignments in Chaar et al., (1987); Burch and Crabb, (1993), magnesium oxide was indicated by the diffraction line at 2θ equal 50° (d spacing of 2.11 Å), whereas the existence of magnesium orthovanadate was indicated by the lines at 2θ equal 34° and 43° (d spacings of 3.04 and 2.44 Å). Employing the Scherrer equation, the diffraction line at 2θ equal 50° was used to estimate the average crystallite sizes for the fresh and the used catalysts. Generally, the crystallite sizes of the used catalysts were larger than those of the fresh catalyst (7.0 nm); they were 15.9, 15.0, 16.0, and 14.4 nm after the catalytic tests at 10,000, 8000, 6000, and 4000 h^{-1}, respectively, which indicate possible morphological changes after the catalytic testing. To investigate this, SEM experiments were performed on the fresh and the used catalysts. As shown in Fig. 7, the morphology of the used catalysts (Fig. 7b and c) was different from that of the fresh catalyst (Fig. 7a). The micrograph of the fresh catalyst exhibited a rough surface with small platelets. These features were not shown by the SEM images of the used catalyst; instead, a less porous surface and large plates can be seen in the micrographs of the used catalysts. Worth noting, these morphological changes are more manifested after the catalytic tests at the GHSV of 4000 h^{-1}. This is consistent with the suggestion by Schmidt et al. that combustion reactions are likely to induce more changes on the catalysts (Schmidt et al., 1994); the catalytic tests at this GHSV consistently showed the highest formation of carbon oxides (Fig. 4).

4. Conclusions

The dehydrogenation of *n*-octane over the VMgO catalyst at the GHSV of 8000 h^{-1} gave the best selectivity to octenes, and that at 6000 h^{-1} showed the highest selectivity to C8 aromatics at high temperatures (500 and 550 °C). However, selectivity to C8 aromatics was comparable over this catalyst at the GHSVs of 6000, 8000, and 10,000 h^{-1} at lower temperatures (400 and 450 °C). The catalytic testing at a GHSV of 4000 h^{-1} showed the lowest selectivity to both octenes and C8 aromatics, which coupled with the highest carbon oxides formation. Moreover, the lowest selectivities for these carbon oxides were observed for the tests at the GHSVs of 6000 and 8000 h^{-1}. The formation of cracking products was significant only at high temperatures (500 and 550 °C). The highest yields for 1-octene (2.6%) and for styrene (3.7%) were obtained for the catalytic tests at the GHSV of 6000 h^{-1}. No phasic changes were recorded after the catalytic tests, but morphological changes, however, were observed.

Acknowledgements

The authors acknowledge the financial support from the National Research Foundation (NRF) and THRIP (South Africa). Thanks also go to the University of KwaZulu-Natal (South Africa) and the University of Khartoum (Sudan).

References

Bhasin, M.M., McCain, J.H., Vora, B.V., Imai, T., Pujado, P.R., 2001. Dehydrogenation and oxydehydrogenation of Paraffins to olefins. Appl. Catal. A: Gen. 221, 397–419.

Blasco, T., Lopez Nieto, J.M., 1997. Oxidative dehydrogenation of short chain alkanes on supported vanadium oxide catalysts. Appl. Catal. A: Gen. 157, 117–142.

Blasco, T., Lopez Nieto, J.M., Dejoz, A., Vazquez, M.I., 1995. Influence of the acid-base character of supported vanadium catalysts on their catalytic properties for the oxidative dehydrogenation of *n*-butane. J. Catal. 157, 271–282.

Bowker, M., 1998. The basis and applications of heterogeneous catalysis. Oxford University Press, pp. 1–22.

Burch, R., Crabb, E.M., 1993. Homogeneous and heterogeneous contributions to the oxidative dehydrogenation of propane on oxide catalysts. Appl. Catal. A: Gen. 100, 111–130.

Chaar, M.A., Patel, D., Kung, M.C., Kung, H.H., 1987. Selective oxidative dehydrogenation of butane over V-Mg-O catalysts. J. Catal. 105, 483–498.

Dejoz, A., Lopez Nieto, J.M., Marquez, F., Vazquez, M.I., 1999. The role of molybdenum in Mo-doped V-Mg-O catalysts during the oxidative dehydrogenation of *n*-butane. Appl. Catal. A: Gen. 180, 83–94.

Elkhalifa, E.A., Friedrich, H.B., 2010. Oxidative dehydrogenation of *n*-octane using vanadium-magnesium oxide catalysts with different vanadium loadings. Appl. Catal. A: Gen. 373, 122–131.

Elkhalifa, E.A., Friedrich, H.B., 2011. On the effect of hydrocarbon/oxygen ratios during the dehydrogenation of *n*-octane over a VMgO catalyst. Catal. Lett. 141, 554–564.

Elkhalifa, E.A., Friedrich, H.B., 2014. Oxidative dehydrogenation and aromatization of *n*-octane over VMgO catalysts obtained by using different MgO precursors and different precursor treatments. J. Mol. Catal. A: Chem. 392, 22–30.

Fung, J., Wang, I., 1991. Dehydrocyclization of C6–C8 n-paraffins to aromatics over TiO_2–ZrO_2 catalysts. J. Catal. 130, 577–587.

Hodnett, B.K., 2000. Heterogeneous Catalysis Oxidation: Fundamental and Technological Aspects of the Selective and Total Oxidation of Organic Compounds. Wiley, pp. 65–101.

Jongpatiwut, S., Sackamduang, P., Rirksomboon, T., Osuwan, S., Resasco, D.E., 2003. *N*-Octane aromatization on a Pt/KL catalyst prepared by vapour-phase impregnation. J. Catal. 218, 1–11.

Kung, H.H., Michalakos, P.M., 1993. Catalytic Selective Oxidation. In: ACS Symposium Series, Washington DC, pp. 389–408.

Mamedov, E.A., Cortes Corberan, V., 1995. Oxidative dehydrogenation of lower alkanes on vanadium oxide-based catalysts. The present state of the art and outlooks. Appl. Catal. A: Gen. 127, 1–40.

Meriaudeau, P., Thangaraj, A., Naccache, C., Narayanan, S., 1994. Aromatization of *n*-octane over Pt-based catalysts: Influence of the support on the product distribution among C_8 aromatics. J. Catal. 146, 579–582.

Schmidt, L.D., Huff, M., Bharadwaj, S.S., 1994. Catalytic partial oxidation reactions and reactors. Chem. Eng. Sci. 49, 3981–3994.

Shi, B., Davis, B.H., 1995. Dehydrocyclization of *n*-octane: H/D exchange and reversible adsorption for a Pt–Sn–SiO_2 catalyst. J. Catal. 157, 626–630.

Sivasanker, S., Padalkar, S.R., 1988. Mechanism of dehydrocyclization of *n*-alkanes over platinum-alumina catalysts. Appl. Catal. 39, 123–126.

Szechenyi, A., Solymosi, F., 2006. *N*-Octane aromatization on Mo_2C-containing catalysts. Appl. Catal. A: Gen. 306, 149–158.

Thomas, J.M., Thomas, W.J., 1997. Principles and Practice of Heterogeneous Catalysis. VCH Weinheim, Germany, pp. 319–415.

Trunschke, A., Hoang, D.L., Radnik, J., Brzezinka, K.-W., Bruckner, A., Lieske, H., 2001. Transition metal oxide/carbon composite catalysts for *n*-alkane aromatization: Structure and catalytic properties. Appl. Catal. A: Gen. 208, 381–392.

Please cite this article in press as: Elkhalifa, E.A., Friedrich, H.B. Oxidative dehydrogenation of *n*-octane over a vanadium–magnesium oxide catalyst: Influence of the gas hourly space velocity. Arabian Journal of Chemistry (2015), http://dx.doi.org/10.1016/j.arabjc.2015.03.017